Wind Tunnel Simulation of Atmospheric Boundary Layer Flows

P. H. A. Barbosa

M. Cataldi

A. P. S. Freire

Mechanical Engineering Program
(PEM/COPPE/UFRJ)
C.P. 68503
21945-970 Rio de Janeiro. Brazil

The present work shows how thick boundary layers can be produced in a short wind tunnel with a view to simulate atmospheric flows. Several types of thickening devices are analysed. The experimental assessment of the devices was conducted by considering integral properties of the flow and the spectra: skin-friction, mean velocity profiles in inner and outer co-ordinates and longitudinal turbulence. Designs based on screens, elliptic wedge generators, and cylindrical rod generators are analysed. The paper describes in detail the experimental arrangement, including the features of the wind tunnel and of the instrumentation. The results are compared with experimental data published by other authors and with naturally developed flows.

***Keywords**: Turbulence, wind tunnel, elliptic wedge generators, roughness, boundary layer, atmospheric flows*

Introduction

The simulation of atmospheric flows in wind tunnels is particularly useful to investigate the effects of shear generated turbulence in the surface layer and of topography and non-uniform wall heat flux on the structure of the flow, including the turbulent transport processes. Of course, wind tunnel operating ranges depend on the dimensions of the tunnel itself, on the dimensions of any simulated environment, on the flow speed and turbulence properties and on the characteristics of the measurement instrumentation.

For studies related to the dispersion of air pollution, frequently the effects of thermal stratification must be considered. It is a plain fact that thermal stratification plays a major role in pollution diffusion in the actual atmosphere and often hazardous environmental conditions arise as a result of, for example, a strongly stable layer created after sunset in the winter; this layer traps down low-level emission.

Because stratified boundary layer flows are normally difficult and expensive to create, many studies have been conducted under adiabatic or neutrally stable conditions. In fact, it has been shown by Poreh et al. (1991) that the minimum length necessary to satisfy most of the requirements of a thermally stratified wind tunnel is a 10 meters long test section.

With a view to construct a short thermally stratified wind tunnel, the Laboratory of Turbulence Mechanics of COPPE/UFRJ has undertaken a series of recent actions. In a preliminary effort, a wind tunnel with a 5 meters long test section was designed and built. The tunnel is fitted with 2 heating panels at the floor and 10 electric heater plates distributed transversally to the flow and parallel to the floor.

The objective of the present work is to show the preliminary tests that have been conducted to qualify the dynamic properties of the produced velocity boundary layer. In normal conditions, for the present wind tunnel geometry, the resulting boundary layer would achieve a maximum thickness of about 4 cm. Thus, a procedure had to be developed to artificially create a thick turbulent boundary layer on the bottom surface of the tunnel.

Thick boundary layers can be created through several artifices; for instance, the paper of Hunt and Fernholz (1975) lists ten possible methods of simulation of neutral, stable and unstable atmospheric conditions in various types of wind tunnel. These methods vary greatly in sophistication and in working principle so that their full understanding and applicability has not as yet been unveiled.

An apparently simple way of generating a thick boundary layer is to force the flow to pass through a combination of spires, wedges or trips together with roughness elements distributed on the wall. From the 28 wind tunnels scrutinised by Hunt and Fernholz (1975), 11 resort to vorticity generators, 23 to roughness elements and 15 to fences. In fact, 9 facilities resort to a combination of all these three simulation methods; this only emphasises their importance.

Unfortunately, since these popular simulation methods are complicated enough from a fluid mechanics point of view, they have encouraged researchers to choose an adequate geometry by trial and error. The works of Counihan(1969) and of Ligrani et al. (1979, 1983), for example, describe thickening devices, which are neatly built with a very sophisticated geometry that requires fine mechanics to be manufactured. Their construction, therefore, is time consuming and frequently costly. This fact is much aggravated by the uncertainty related to their applicability in a different wind tunnel environment from that to which they were originally designed.

In a previous work, Guimarães et al. (1999) have shown how a combination of spires and trips can be used to produce thick boundary layers with characteristics similar to the atmospheric boundary layer. Five different geometrical arrangements were presented to produce boundary layers of thickness varying from 9 to 18 cm. The geometries were much simpler than those presented by Counihan (1969) and by Ligrani et al. (1979, 1983) resulting from simple geometric compositions made with rods and bars. The boundary layer was qualified by examining the following features: growth, structure, equilibrium and turbulent transport of momentum.

The main contribution of this work is to extend the results of Guimarães et al. (1999) to a further range of validity. In addition, different types of geometry will be tested. Thus the work aims at producing artificial boundary layers with thickness up to 27 cm and good qualification properties. More than that, the work aims at producing boundary layers with a higher quality than those presented in Guimarães et al. (1999); boundary layers that present properties closer to a naturally developed boundary layer in relation to the qualification parameters described above and also in relation to the longitudinal spectrum.

Next, a short review on the techniques used to thicken the boundary layer will be presented. Then, the experimental apparatus and procedure will be described. The experimental results and comparison with other works are given in section four.

Simulation Methods

As mentioned by Hunt and Fernholz (1975) several techniques have been used to artificially thicken the boundary layer. Typical examples are the use of fences, uniform grids, graded or sheared grids, jets, pulsation, wall roughness, steps, screens, vortex generators and thermal stratification.

Usually, these techniques are divided into three categories:

Article received: July, 2001. Technical Editor: Aristeu da Silveira Neto.

1. Alteration of the surface conditions by the use of roughness or boundary layer trips.

2. Alteration of both the inner and the outer regions of the boundary layer by directional jets placed in the floor at the entrance to the working section or by multiple horizontal jets of variable strength directed at each other from either side of the wind tunnel.

3. Alteration of the external irrotational flow by spires extending all the way from the wall to the oncoming flow. The turbulent wakes formed by the spires convect downstream to merge with the existing boundary layer resulting in a new structure which, in some cases, may resemble a thick boundary layer.

Here, we will use the third procedure to generate a thick boundary layer. Thus, before we move on it is important to establish the physics of the problem.

Kline et al. (1967) has shown that the turbulence structure is primarily defined by the turbulence production rate. In a normally developed boundary layer the overall structure results from large scale structures originated from the interaction between eddies formed by near-wall turbulent bursts and by the inflow of high-speed flow towards the wall. The bursts are provoked by a strong instability mechanism and play a fundamental role in transporting turbulent kinetic energy to the outer region of the boundary layer.

Thus, according to this picture, the structure of the flow downstream of the spires results from the mixing between the organised large eddy motion generated by the wakes of the spires and the violent ejection of low-speed fluid from the very near wall regions. Hence, before the flow is likely to conform to the boundary layer properties, a sufficient degree of mixing must be assured to it so that the lifetime of the large eddy wake structures is exceeded.

All the above places emphasis on the idea that the wall layer streak formation and break up play the central role in determining the structure of the turbulent boundary layer and that for this reason the details of the wake flow behind the spires exert a minor role on the process.

The spires designed in the mid sixties were based on completely different principles; they intended to produce a model flow based on the existence of sets of large eddies in both the inner and the outer regions of the boundary layer. Triangular generators with pairs of surfaces at alternate incidences were designed to produce large vortices of opposite sign of the type envisaged by Townsend (1957). These vortices should accelerate the outward diffusion of the high intensity turbulence produced at ground level.

Experiments using triangular generators indicated a tendency for an excessive momentum loss in the inner region of the boundary layer and an insufficient loss in the outer region. In an attempt to resolve this, elliptic generators were developed. Elliptic generators were designed to keep turbulence constant with height or, more acceptable, to produce turbulence levels that decayed from some maximum value near the wall to approximately zero at the edge of the shear flow. The side view of the elliptic wedge generators presented by Counihan (1969) is a quarter ellipse whose major axis is twice the length of the minor axis. The plan view of the generator is wedge shaped; the apex of the wedges faces the flow. Two types of wedges with constant angles of 5° and 6° were tested. The final assessment was based on measurements of the distribution of longitudinal turbulence in the wake of single generators. A span-wise variation of turbulence of the order of 1% was required at any given height in the boundary layer.

Ligrani et al.(1979, 1983) used streamlined spires with sharp-edged upstream and downstream blades. The total angle of the upstream blade was carefully adjusted for a fine-tuning of the fluctuation intensities. A cross barrier set downstream of the spires was used to increase the momentum deficit over that wich resulted from the spires alone.

Experimental Apparatus

In the present work, it was decided that three types of geometrical elements would be considered for the construction of the thickening device. Following the procedure of Counihan (1969), elliptic wedge generators were considered. In reference to the procedure of Guimarães et al. (1999) two other basic components were used: cylindrical rods and rectangular bars.

The shape and location of the components were determined through trial and error. In fact, before we arrived at the definitive geometry, several attempts were made. In our first try, fences were used; they resulted, however, in very distorted velocity profiles. Basically, the aerodynamic drag of the fences was too high so that a strong blockage effect was achieved resulting in a strong acceleration of the flow in the top half of the tunnel.

Elliptic wedge generators were also tried. For that matter, we followed the design proposed by Couhinan (1969) but with a wedge angle of 5.7°. The procedure for an assessment of the properties of the resulting flow was also borrowed from Counihan. The measurements were taken at a distance of 600 mm, i.e. three boundary layers heights, downstream of the generator trailing edges. As we shall see, the agreement between our results and those of that author are very good. However, when data were collected for a distance about 2000 mm downstream of the generators, a flow with an exaggerated wake region was found.

Different combinations of rods and bars were studied to produce many different types of geometries. In all configurations, an array of rods that extended across the width of the wind tunnel was used. Rectangular bars located on the downstream side of the rods (trailing trips) were also used to achieve normal turbulence structure. As the flow approached the rods, a trip was placed over the wall.

The main advantage of this geometry as compared with others was really its simplicity. However, because the rods had a constant diameter, controlling the level of turbulence in distances far away from the floor was very difficult. The general features of the present design were taken from Ligrani et al.(1983), who in turn based their design on an apparatus developed by Cermak (1971), Peterka and Cermak (1974) and Cermak (1975) to simulate the atmospheric boundary layer.

Four geometrical configurations of the thickening apparatuses are shown in Figures 1 to 4.

The thickening apparatuses were tested for just one free stream velocity. The wind tunnel used was the high turbulence wind tunnel located at the Laboratory of Turbulence Mechanics of the Mechanical Engineering Program of COPPE/UFRJ; for flows over a uniformly smooth surface, the free stream level of turbulence was about 2%. The tunnel is an open circuit tunnel with a test section of dimensions 670 x 670 x 5000 mm; the test section has a roof with adjustable inclination to assure the flows to have a zero pressure gradient.

Measurements were performed for values of the free-stream velocity of, approximately, 3.00 m/s. Mean velocity profiles and turbulence intensity levels were obtained using a constant temperature hot-wire anemometer. The probe used was of the type DISA 55P11. A Pitot tube, an electronic manometer, and a computer controlled traverse gear were also used. The uncertainty associated with the velocity measurements was: U = 0.064 m/s precision, 0 bias (P = 0.95).

To obtain accurate measurements, the mean and fluctuating components of the analogic signal given by the anemometer were treated separately. Two output channels of the anemometer were used. The mean velocity profiles were calculated directly from the untreated signal of channel one. The signal given by channel two was 1 Hz high-pass filtered leaving, therefore, only the fluctuating velocity. The latter signal was then amplified with a gain controlled

between 1 and 500 and shifted by an offset so as to adjust the amplitude of the signal to the range of the A/N converter.

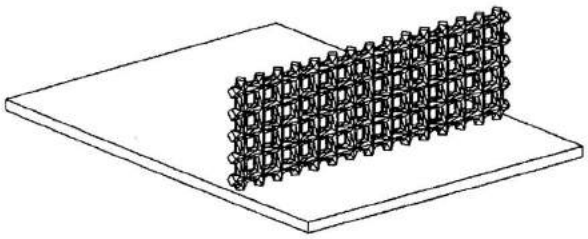

Figure 1. Grid located at the entrance section of the wind tunnel.

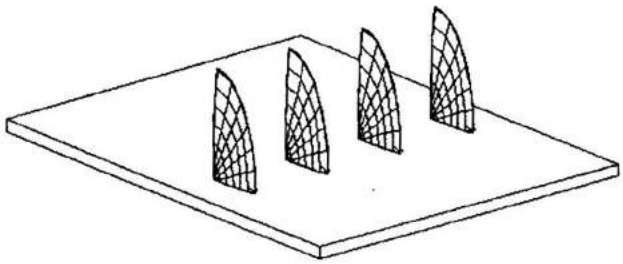

Figure 2. Elliptic wedge generators at the entrance section of the wind tunnel.

Experimental Assessment of the Generators

The assessment was carried out considering the integral properties of the flow, skin-friction, mean velocity profiles in inner and outer co-ordinates and longitudinal spectrum of turbulence.

Elliptic Wedge Generators

In a preliminary study, the elliptic wedge generators were tested individually. Velocity and turbulence intensity profiles were taken at the centreline of the wedge and at several stations at different spanwise distances.

The wedge geometry is exactly that described by Counihan (1969).

The results are shown in Figures 5 to 6. As expected, the generators produced turbulence levels that decayed from some maximum value near the wall to approximately zero at the edge of the shear flow. The notable point here is that, as mentioned by Counihan (1969), at any given height, the spanwise turbulence intensity is sensibly constant over a good proportion of the spanwise extent of the wake. For the final flow profile, it was decided that a spanwise variation of turbulence of the order of 1% would be desirable at any given height. Thus according to Figure 6, a spacing of 90 mm was the most adequate.

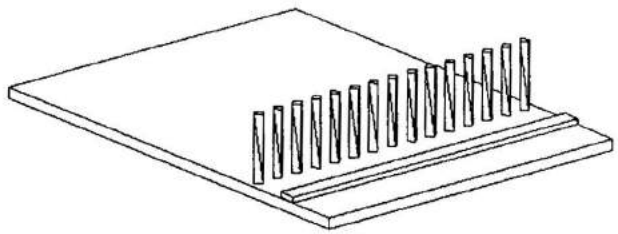

Figure 3. Rods with 80 mm and a leading trip.

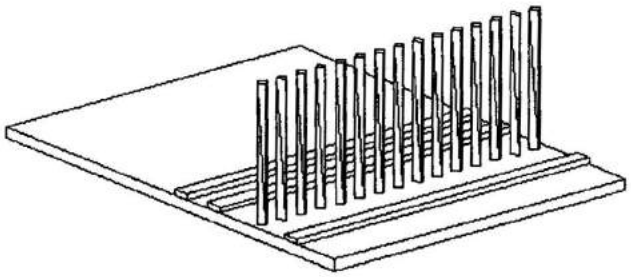

Figure 4. Rods with 160 mm, one leading trip and two trailing trips.

As mentioned in section 3, the overall results for the elliptic wedge generators were good. However, when measurements were taken far downstream from the generators a very pronounced wake region was observed. To rectify this difficulty several alternative configurations were tried with the addition of leading and trailing trips. These trips where made of rectangular (15 mm x 5 mm) aluminium bars that run across the wind tunnel. The velocity profiles in inner and outer variables are shown in Figures 7 and 8. Please note the ill definition of the wake profile. The resulting values of C_f were about 25% below the expected values. The results for the longitudinal spectrum were also not good.

Failure in achieving reasonable results with the elliptic wedge generators prompted the authors to seek an alternative approach. For this reason, we have decided to conduct further experiments with an alternative geometry, based on that described by Guimarães et al. (1999).

Grids

Before experimenting with the rods, some runs were conducted with a uniform grid. The grid was made of 1/8'' diameter wires with a 3/8'' mesh distance. The grid was 30 cm high and spanned the whole working section of the tunnel. Eight different configurations with the grid were tested. The grid always started with a wire lying on the wall. In addition, leading and trailing trips were also considered. Overall the results for the inner region of the boundary layer were not bad as shown in Figure 9. The wake profile, however, was badly distorted (Figure 10). Cf was about 10% above the expected value and the spectra of longitudinal velocity showed good discrimination. The general conclusion here was that although the near wall flow was well resolved, the wake region was poorly defined.

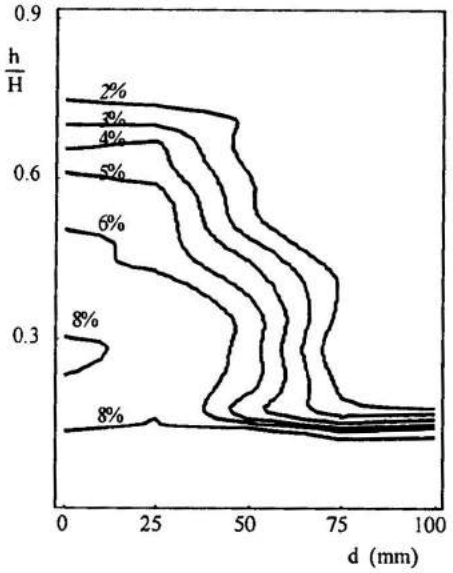

Figure 5. Contours of constant longitudinal turbulence in the wake of the generators according to the normalized probe height (h/H) and the spanwise distance between the probe center line and the wedge generator center line (d). H denotes the height of the generators.

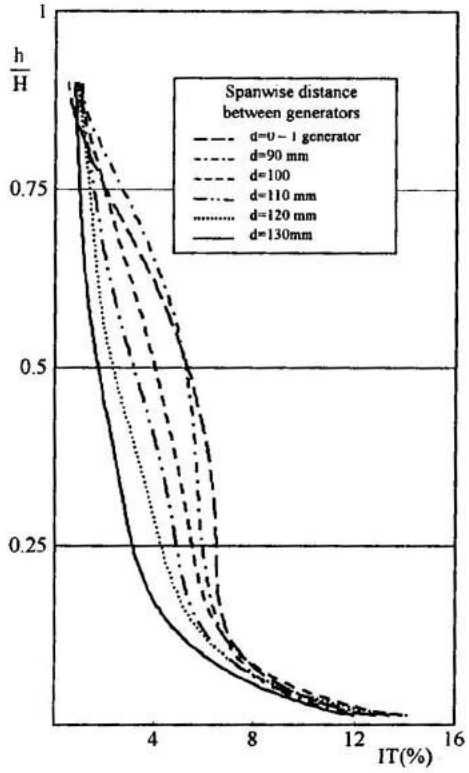

Figure 6. Effect of the generators spacing on the wake distribution of longitudinal turbulence. IT% stands for relative turbulence intensity.

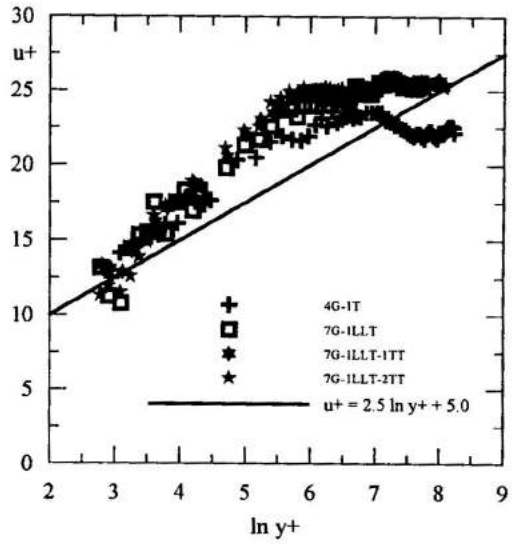

Figure 7. Velocity profiles in inner co-ordinates. Wedge generator geometry. 4G or 7G indicates the number of generators, LLT a large leading trip, TT a trailing trip. u+ = u/utau. y+ = y utau/nu.

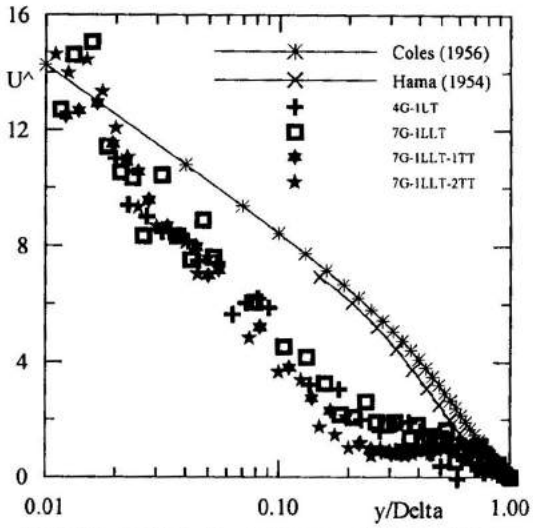

Figure 8. Velocity profiles in outer co-ordinates. Wedge generator geometry. Key to symbols as in Figure 7. U^ = (Uinf – U)/utau.

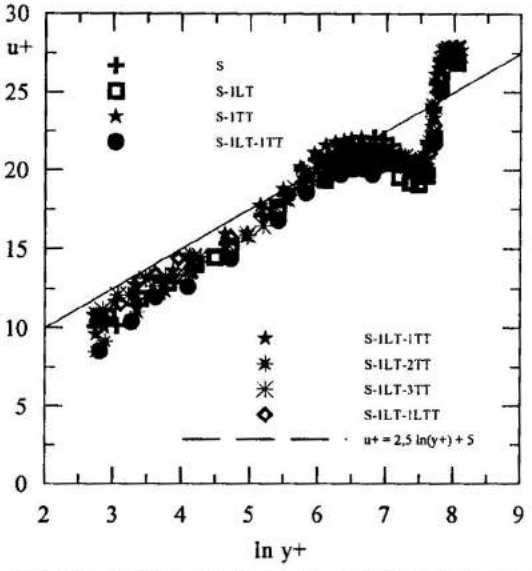

Figure 9. Velocity profiles in inner co-ordinates. Grid geometry. S indicates the grid, LT a leading leading trip, TT a trailing trip and LTT a large trailing trip.

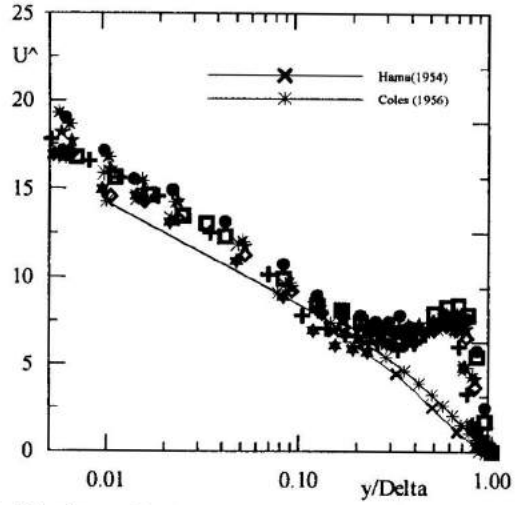

Figure 10. Velocity profiles in inner co-ordinates. Grid geometry. Key to symbols as in Figure 9.

Rods

In Figures 3 and 4, the thickening devices that use rods as their central element are shown in position. The rods were made by cutting cylindrical 1/8" diameter bars in two different heights: 80 mm and 160 mm. In the configuration for the 80 mm rods, an optimal arrangement was found by placing each rod 10 mm apart from each other. In our case, 66 rods were used to achieve the expected effect. Four arrangements with rectangular (15 mm x 5 mm) aluminium bars (trips), transversal to the mean flow, were studied. In all configurations, the leading (trailing) trip was placed 80 mm far upstream (downstream) from the rods as shown in Figures 3 and 4. For the 160 mm rods, an optimal arrangement only was reached when each rod was spaced 7 mm from each other. To achieve this, 95 rods were used. Two identical trips were positioned, respectively, at 80 mm and 150 mm downstream from the rods; also a 1/8" cylindrical bar was placed at different heights.

The velocity profiles in inner and outer variables are shown in Figures 11 to 14. Although the logarithmic regions were well characterised in Figures 11 and 12, the classical law of the wall for smooth surfaces was not obtained here. The level of the straight line that should be equal to 5 was found to be lesser than that. In fact, the velocity profile when written in terms of a power law profile was noted to have an exponent equal to 0.31. This will be discussed next. The spectra are shown in Figures 15 and 16.

The velocity profiles plotted in wall co-ordinates shown in Figures 11 and 13 were prepared with values of C_f obtained through the graphical method of Clauser, that is, through the inclination of the velocity profile in the fully turbulent region of the flow.

In all cases they were compared with the classical law of the wall formulation

$$\frac{u}{u_\tau} = \frac{1}{k}\ln\left(\frac{y u_\tau}{\nu}\right) + A \qquad (1)$$

where k=0.4 and A=5.0.

For large values of ($y u_\tau / \nu$), the velocity departs from the law of the wall giving form to the law of the wake (Coles (1956)). In wake co-ordinates, the velocity profiles show good agreement with the law of the wake of Coles (Figures 12 and 14). They were also approximated by a power-law variation. The resulting value for the exponent, n is shown in Table 2 compared with wind data collected from 19 different sites as presented by Davenport (1960, 1963).

Qualification of the artificially thickened boundary layer included the spectra of the longitudinal velocity fluctuations. The one-dimensional spectra were calculated considering Taylor's hypothesis. Thus, the equation for the local wave number spectrum was written as

$$E(k) = \frac{4\overline{u^2}}{\overline{U}} \int_0^\infty F(x)\cos(kx)dx \qquad (2)$$

where k denotes the one-dimensional wave number.

Results were compared with Kolmogorov's law where the Fourier operator is written as

$$F(x) = \alpha \varepsilon^{2/3} k^{-5/3}$$

ε is the dissipation rate by mass unit and k is the wave number.

As can be observed in Figures 15 and 16, the longitudinal turbulence spectra for all stations seem to be in a good agreement with the Kolmogorov's empirical $k^{-5/3}$ decay law. It can also be noted that, except at station 1, as the downstream distance from the thickening device increases, the energy peak increases too. Actually, this fact has also been observed by other authors.

At station 1, the flow did not achieve a sufficient degree of mixing to produce a thick boundary layer profile with normal properties. The same behaviour was confirmed when mean velocity profiles were plotted in both inner and outer co-ordinates for rods with 80 and 160 mm.

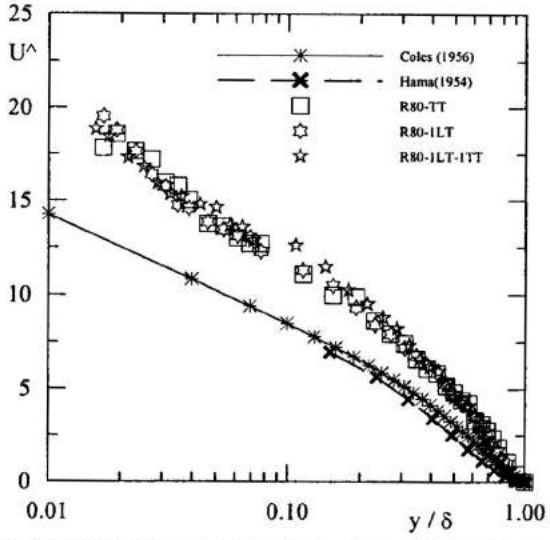

Figure 11. Velocity profiles in inner co-ordinates. Rods with 80 mm. LT indicates a leading trip, TT a trailing trip.

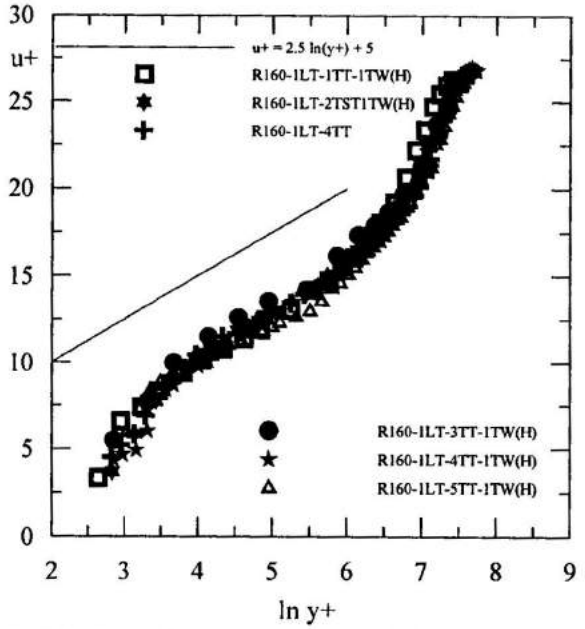

Figure 12. Velocity profiles in inner co-ordinates. Rods with 160 mm. LT indicates a leading trip, TT a trailing trip. TW a transversal wire placed at height H.

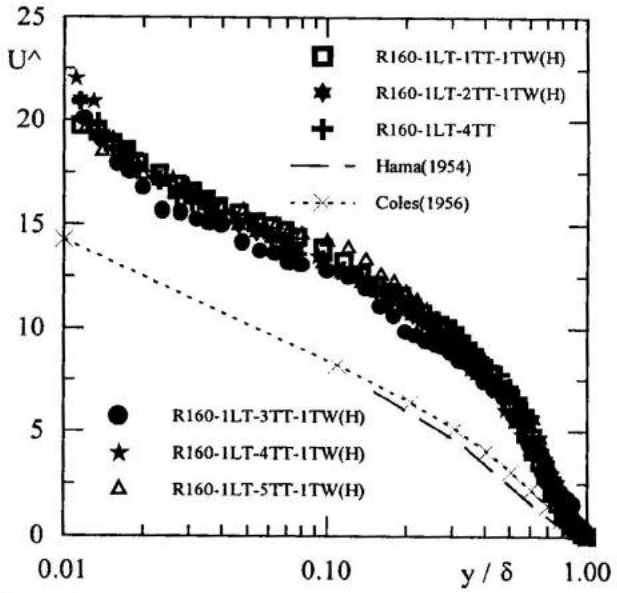

Figure 14. Velocity profiles in outer co-ordinates. Rods with 160 mm.

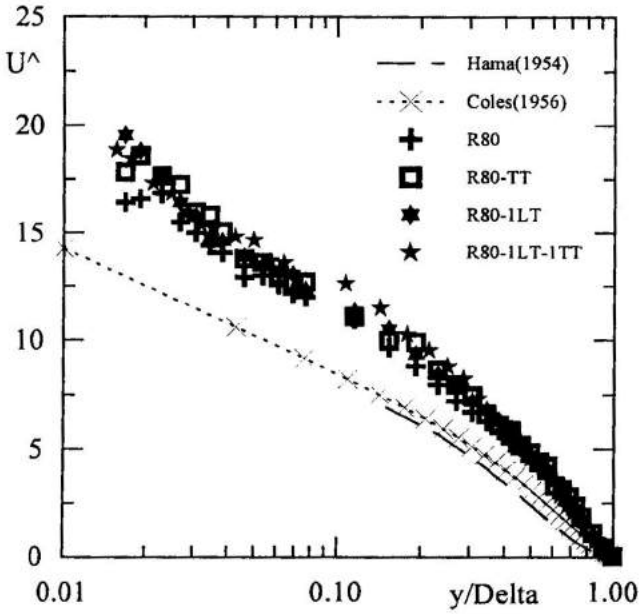

Figure 13. Velocity profiles in outer co-ordinates. Rods with 80 mm.

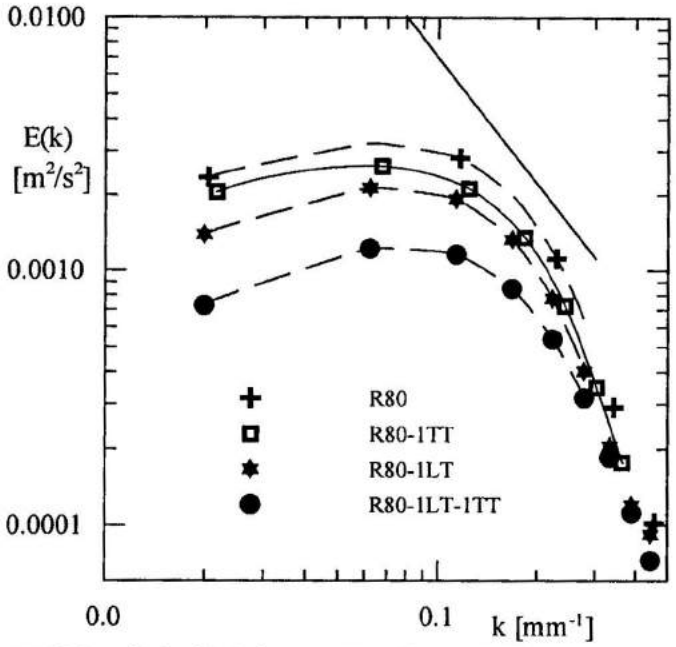

Figure 15. Longitudinal turbulence spectra. Rods with 80 mm. Straight line indicates Kolmogorov's power law.

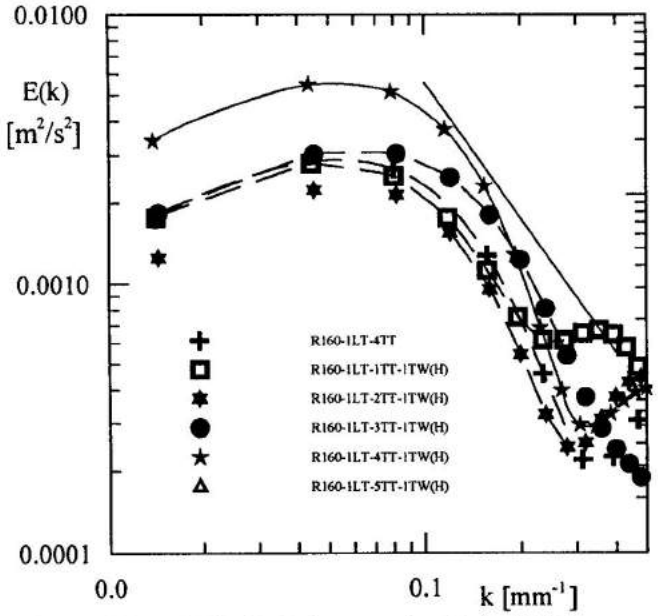

Figure 16. Longitudinal turbulence spectra. Rods with 160 mm.

Integral Properties

The boundary layer growth can be characterised through the variation with the downstream distance of the momentum thickness, the skin-friction coefficient and the Clauser parameter.

The momentum thickness was evaluated directly from the mean velocity profile through a simple numerical quadrature. The results are shown in Figure 17 for the geometric configurations involving the rods and the bars. The effective velocity boundary layer origin was then determined based on the momentum thickness correlation:

$$\delta_2 = 0.036x\left(\frac{U_\infty x}{\nu}\right)^{-1/5} \tag{3}$$

The extent in origin is shown in Table 1. The extent in origin represents the distance that a naturally developed boundary layer would need to flow so that its properties would achieve the values measured here.

The calculated skin-friction results are shown in Figure 18. The values of C_f were determined directly from the velocity profiles through the gradient of the logarithmic profile. The data are also shown compared with $C_f/2 = 0.0128\ Re_{\delta_2}$.

Table 1. Upstream extent in origin.

Configuration	*Station (mm)*	*Origin Location*
RODS (80 mm)	2100	8.75 m
	2200	8.66 m
	2300	8.64 m
	2400	8.57 m
RODS (160 mm)	4100	25.49 m
	4200	21.60 m
	4300	25.09 m
	4400	23.18 m

The Clauser shape factor G, defined as

$$G = \frac{\int_0^\infty \frac{U_\infty - U}{u_\tau} dy}{\int_0^\infty \left(\frac{U_\infty - U}{u_\tau}\right)^2 dy} \tag{4}$$

was found to be nearly constant and about 8 for the 80 mm rods and about 10 for the 160 mm rods. Indeed, for most configurations, the experimental value of G was found to lie about a constant value.

Data Analysis

Table 2, which was first shown in Guimarães et al. (1999), is here presented again; it contains a comparison between our results and data obtained in other wind tunnels. In addition, some atmospheric boundary layer features from three different natural flow conditions are listed too.

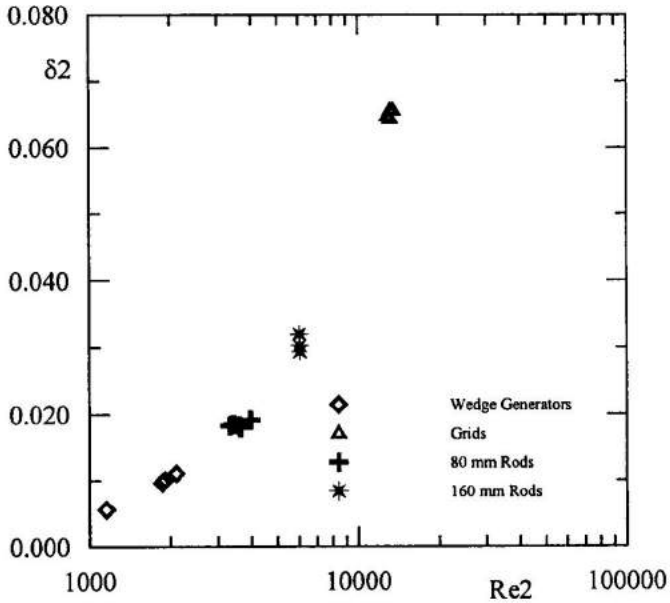

Figure 17. Momentum thickness. Re2 stands for the Reynolds number based on the momentum thickness.

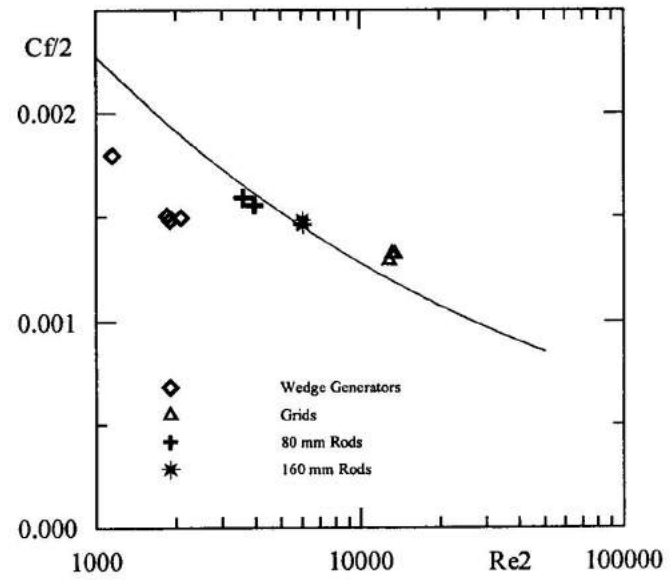

Figure 18. Skin-friction coefficient. Re2 stands for the Reynolds number based on the momentum thickness. The straight line denotes values for a naturally developed boundary layer.

Table 2. Wind tunnel simulation systems and ABL features.

Institution	*W-T dimensions (m)*	*S.M.*	*M.S./F.S*	$\delta(m)$	*n*	u_τ/U_∞	*IT%*
Vienna	1.7 x 1.2 x 10	F, R	1/200	0.6	–	–	–
Bochum	2.1 x 2.1 x 4.3	F, V, R	1/500	0.84	–	–	–
Marseille	3.2 x 1.5 x 40	R, T	1/20	0.75	–	0.045	2.0
Poitiers	5.5 x 5.3 x 26	GG, R, T	1/200	2.5	–	–	–
Edinburgh	1.5 x 0.9 x 9	V, Sc, R	1/350	0.7	0.36	0.050	1.8
Salford	0.5 x 0.5 x 1	UG, GG, Sc	–	0.4	–	–	–
Stevenage	4.3 x 1.5 x 22	F, V, R	1/50	1.0	–	0.055	1.8
Notre Dame	1.5 x 1.5 x 14	J, R, T	1/100	1.0	–	0.044	3.1
COPPE/UFRJ	0.67 x 0.67 x 5	Sc, V, R, T	–	0.27	0.31	0.048	2.0
Rural A.B.L.	–	–	–	500	0.16	0.030	2.6
Urban A.B.L.	–	–	–	600	0.40	0.050	2.6
Over Sea A.B.L.	–	–	–	280	0.15	–	8.0

Key to table: W-T – wind tunnel; S.M. – simulation method; M.S./F.S. – model scale over full scale; n – exponent of the power-law profiles; A.B.L. – atmospheric boundary layer; F – fences; R – roughness; V – vortex or vorticity generators; GG – graded or shear grids; UG – uniform grids; Sc – screens; T – thermal stratification; J – jets.

Our experimental data will now be compared with the neutral boundary layer data of Mickle et al.(1988). To that end, first we have to re-write the law of the wall as

$$\frac{u}{u_\tau} = \frac{1}{k}\ln\left(\frac{y}{y_0}\right) \qquad (5)$$

Then a direct comparison between equations (1) and (5) allows y_0 to be evaluated from the known values of u_τ and A. For our experimental data, y_0 = 3 cm. The resulting graphs for the velocity profiles in inner and outer co-ordinates are shown next in Figures 19, 20 and 21.

Conclusions

As corroborated by the data presented in the previous sections, the results obtained at the high-turbulence wind tunnel located at COPPE/UFRJ stand reasonably well against a comparison with wind tunnel data published by other authors and with data obtained for natural flow. The main contribution of the work has been to identify a simple geometrical arrangement that is capable of generating thick turbulent boundary layers with properties very close to normal properties.

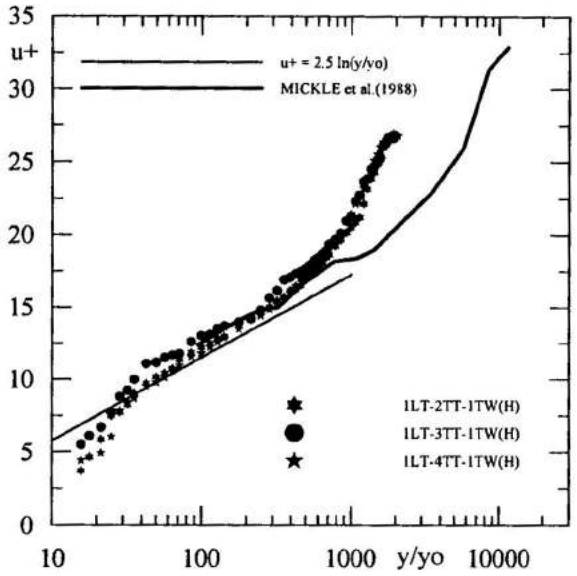

Figure 19. Comparison with the data of Mickle et al.(1988). Velocity profiles in inner co-ordinates. Rods with 160 mm. LT indicates a leading leading trip, TT a trailing trip. TW a transversal wire placed at height H.

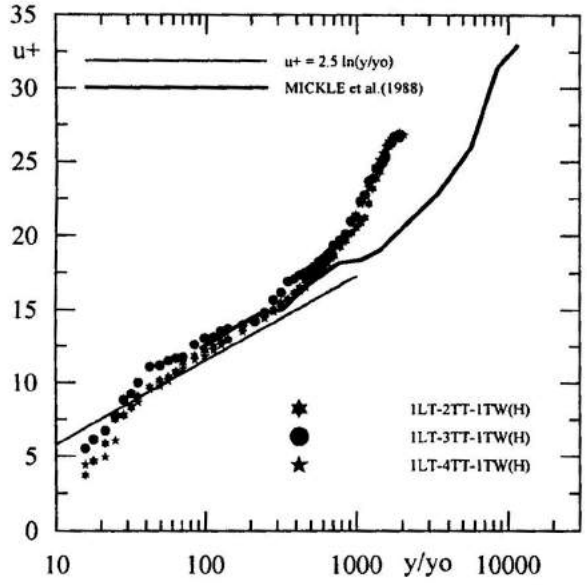

Figure 20. Comparison with the data of Mickle et al.(1988). Velocity profiles in outer co-ordinates. Rods with 160 mm. LT indicates a leading leading trip, TT a trailing trip. TW a transversal wire placed at height H.

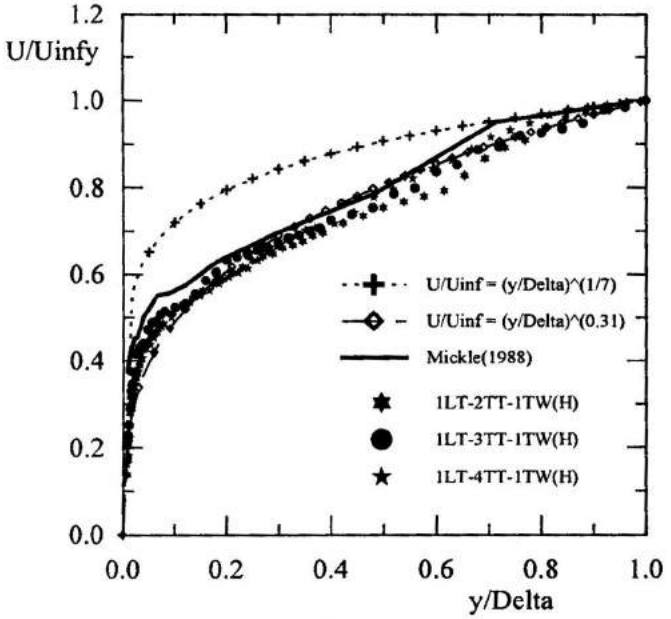

Figure 21. Comparison with the data of Mickle et al.(1988). Velocity profiles in outer co-ordinates. Rods with 160 mm. LT indicates a leading leading trip, TT a trailing trip. TW a transversal wire placed at height H.

The task of reproducing in a laboratory the features of the atmospheric boundary layer is a very difficult problem that demands time and resources. In a previous work, Guimarães et al. (1999) have achieved qualified boundary layers with up to 14 cm thickness. Here we have further extended this range to 27 cm. When this work started out the objective was to produce qualified boundary layers with a thickness of 40 cm. Unfortunately, with the previous working section 3000 mm long, only thickness up to 16 cm could be obtained. The goal of obtaining thicker boundary layers then prompted us to increase the length of the working section to 5000 mm. In fact, when the first velocity profiles were obtained for the 16 mm rods, the defect region of the boundary layer presented a deficit in velocity which was thought by the present authors to be excessive. To correct this effect the test section of the wind tunnel was extended from 3000 mm to 5000 mm. After experimental verification, it was in fact confirmed that the additional 2 meters were sufficient for a further mixing of the flow to conform the boundary layer to the desired properties.

Acknowledgements

The present work was financially supported by the Brazilian National Research Council -- CNPq -- through grant No 523476/96-5. A short version of this paper was considered the best paper presented at the Micrometeorology Section in the Congress of Brazilian Meteorological Society, held in Rio de Janeiro in October 2000.

References

Cermak, J. E.; 1971, Laboratory simulation of the atmospheric boundary layer, A.I.A.I. J., vol. 9, pp. 1746.

Cermak, J. E.; 1977, Applications of fluid mechanics to wind engineering - A Freeman Scholar Lecture, J. Fluids Engineering, vol. 97, pp. 9.

Coles, D.; 1956, The law of the wake in turbulent boundary layer, J. Fluids Mechanics, vol. 1, pp. 191-226.

Counihan, J.; 1969, An improved method of simulating an atmospheric boundary layer in a wind tunnel, J. Fluid Mechanics, vol. 3, pp. 197-214.

Davenport, A. G.; 1960, A rationale for determination of design wind velocities, Proceedings of Conference on Buildings and Structures, N.P.L., U.K., pp. 54-83.

Davenport, A. G.; 1963, The relationship of wind structure to wind loading, Proceedings ASCE, Journal of the Structural Division, vol. 86, pp. 39-66.

Guimarães, J. H. D., dos Santos, S. J. F., Jr., Su, J. and Silva Freire, A. P.; 1999, Large artificially generated turbulent boundary layers for the study of atmospheric flows, Proceedings of the 15th Brazilian Congress of Mechanical Engineering (COBEM99), Águas de Lindóia.

Hunt, J. C. R. and Fernholz, H.; 1975, Wind-tunnel simulation of the atmospheric boundary layer: a report on Euromech 50, J. Fluid Mechanics, vol. 70, pp. 543-559.

Kline, S. J., Reynolds, W. C., Schraub, F. A. and Runstadler, P. W.; 1967, The structure of turbulent boundary layer, J. Fluid Mechanics, vol. 30, pp. 741-773.

Ligrani, P. M., Moffat, R. J. and Kays, W. M., 1979, The thermal and hydrodynamic behavior of thick rough-wall turbulent boundary layers, Report No HMT-29, Stanford University.

Ligrani, P. M., Moffat, R. J. and Kays, W. M., 1983, Artificially thickened turbulent boundary layers for studying heat transfer and skin-friction on rough surfaces, J. Fluids Engineering, vol. 105, pp. 146-153.

Mickle, R. E., Cook, N. J., Hoff, A. M., Jensen, N. O., Slamon, J. R., Taylor, P. A., Tetzlaff, G. and Teunissen, H. W.; 1988, The Askervein hill project: Vertical profiles of wind and turbulence, Bound. Layer. Meteor., vol. 43, pp. 143-169.

Poreh, M., Rau, M. and Plate, E. J.; 1991, Design considerations for wind tunnel simulations of diffusion within the convective boundary layer, Atmospheric Environment, vol. 25A, No 7, pp. 1251-1256.

Peterka, J. A. and Cermak, J. E; 1974, Simulation of atmospheric flows in short wind tunnel test sections, CER 73-74JAP-JEC2, Fluid Mechanics Program, Colorado State University.

Townsend, A. A.; 1957, The turbulent boundary layer, Proc. I.U.T.A.M. Symposium on Boundary Layer Research, Springer, Berlin.

